Super-resolution critical dimension limits of positive tone i-line photoresists

David B. Miller, Adam M. Jones, Robert R. McLeod

David B. Miller, Adam M. Jones, Robert R. McLeod, "Super-resolution critical dimension limits of positive tone i-line photoresists," Proc. SPIE 10544, Advanced Fabrication Technologies for Micro/Nano Optics and Photonics XI, 105440N (22 February 2018); doi: 10.1117/12.2287470

SPIE.

Event: SPIE OPTO, 2018, San Francisco, California, United States

Super-Resolution Critical Dimension Limits of Positive Tone i-line Photoresists

David B. Miller[1*], Adam M. Jones[2], Robert R. McLeod[1]
[1]*Electrical, Computer and Energy Engineering Department, University of Colorado, Boulder, Colorado 80309, USA*
[2]*Sandia National Laboratories, Albuquerque, New Mexico, 87123, USA*
* dbmiller@colorado.edu

ABSTRACT

Applying a technique borrowed from super-resolution microscopy to photolithography, we achieve critical dimensions well below the diffraction limit. Exposing photoresist in the far-field, over a broad area, we can demonstrate dimensions as small as λ/7. In this paper, we show that conventional i-line photoresists exposed with this technique, along with modified processing, are capable of supporting features as small as 50 nm, and possibly smaller. We consider the necessary requirements to achieve sub-diffraction dimensions, detail a simple model for photoresist development, and show its use in predicting the minimum attainable feature size. Finally, we characterize two commercial photoresists, and compare the resulting features to those of the model.

Keywords: Super-resolution Lithography, Nanolithography, Interference Lithography, I-line Lithography, Resist Characterization

1. INTRODUCTION

In this paper, we show that sub-diffraction limited critical dimensions (CDs) in conventional i-line photoresists are possible with far-field, large area, i-line (λ = 365nm) exposure tools. In addition, we explore the necessary requirements to achieve sub-diffraction limited critical dimensions. Finally, we characterize two commercial off the shelf photoresists, and use those parameters to determine the ultimate capabilities of each resist. With standard i-line photoresists, we have achieved patterns with feature sizes down to 50 nm; more than seven times below the wavelength used in i-line exposure tools. In comparison to existing nanofabrication methods, such as e-beam lithography, sub-diffraction photolithography has two distinct advantages. First, photolithography throughput is orders of magnitude larger than e-beam lithography. Second, photolithography can be scaled up to pattern areas much larger than the limits imposed by e-beam stage accuracy. By reducing the achievable feature size of near UV sources and commercial photoresists to the 50 nm scale, this method enables nanofabrication without the cost and complexity of deep UV immersion photolithography steppers.

Photolithography is used in the fabrication of all microelectronics. An image of the pattern (the aerial image) is projected into a light sensitive polymer (photoresist), and the polymer is then chemically developed to leave behind the exposed pattern (latent image). Positive tone photoresists, the focus of this work, are removed upon development in the regions exposed to light. After developing, this remaining patterned photoresist layer serves as a mask while processing the underlying substrate. Lithographic resolution is defined as the minimum separation between uniquely resolvable features, and is diffraction limited[1]. Critical dimensions, on the other hand, relate to the width of individual features within a pattern. As the response of the photoresist is non-linear, critical dimensions are not necessarily limited by diffraction. Typically, lithographic resolution is improved by decreasing the exposure wavelength λ, and increasing the NA, as described by the well-known expression[1]:

$$R = K\frac{\lambda}{NA} \tag{1}$$

Current exposure tools have been stuck at a λ = 193 nm, although EUV tools (λ = 13 nm) have been promised for some time[1]. Numerical aperture has been increased through improved lens design, as well as immersion techniques. Both strategies come with challenges, as well as increased tool costs.

We achieve sub-diffraction limited critical dimensions by applying a technique from super-resolution microscopy to photolithography. Stimulated emission depletion (STED) microscopy uses a high-contrast dark null in a Gauss-Laguerre beam to localize fluorescence within the small central region of the null. Imaging at the scale[2] λ/100 is

Advanced Fabrication Technologies for Micro/Nano Optics and Photonics XI, edited by Georg von Freymann, Winston V. Schoenfeld, Raymond C. Rumpf, Proc. of SPIE Vol. 10544, 105440N · © 2018 SPIE
CCC code: 0277-786X/18/$18 · doi: 10.1117/12.2287470

possible because of the non-linear response of fluorophores and high optical contrast. Taking advantage of the non-linear response of photoresists and high optical contrast, we apply a similar concept to photolithography. Projecting and overexposing a high contrast aerial image leaves only the darkest regions unexposed, and subsequently undeveloped. Resulting pattern linewidth then decreases as the square root of exposure dose, as is the case for STED[3]. Unlike single-point STED, here a large area pattern can be projected, only constrained to having individual features separated by the diffraction limit. Standard multiple-patterning lithography methods can then be applied to fabricate arbitrary patterns with both critical dimension and feature spacing below the diffraction limit[4].

A key requirement for extending i-line photolithography to smaller features, is photoresist which is able to support these feature sizes while remaining compatible with i-line lithography tools. To test the suitability of commercially available resists with this patterning approach, we use interference lithography as a test platform. Interference lithography is a mask-less exposure technique used to generate a high contrast, diffraction limited, periodic pattern over a large area. By interfering two mutually coherent beams, alternating bright and dark regions are formed. The pitch of the pattern Λ, is determined by wavelength λ and angle of interference θ (*Equation 2*). For interference lithography, aerial image contrast *M,* defined in *Equation 3*, is the interference fringe contrast. The interference contrast is set by the mutual coherence of the interfering beams. Perfect contrast, $M = 1$, is only achieved when the interfering beams are fully coherent. Therefore, it is important that both the spatial and temporal coherence be sufficient for high image contrast across the full exposure field.

$$\Lambda = \frac{\lambda}{2\sin(\theta)} \tag{2}$$

$$M = \frac{I_{max} - I_{min}}{I_{max} + I_{min}} \tag{3}$$

We demonstrate sub-diffraction limited critical dimensions in two different positive tone i-line photoresists, Ultra-i and AZ 4210. We demonstrate 50 nm features in Ultra-i, a photoresist optimized for critical dimensions of 250 nm. Additionally, we also show that even workhorse resists not optimized for sub-micron features, such as AZ 4210, can be extended to work at length scales below 100 nm. We demonstrate 80 nm features in AZ 4210, more than an order of magnitude smaller than the specified critical dimension of one micron.

2. RESIST DEVELOPMENT MODEL

We use a simple two threshold resist development model[5], shown qualitatively in *Figure 1*, and quantitatively in *Equation 4* below. Here, threshold D_1 is the maximum exposure dose which will not initiate development. Threshold D_2 is the minimum exposure dose which will allow complete development. The remaining film thickness, T_{norm}, is normalized to the initial film thickness. The two model parameters D_1 and D_2 are readily determined by experiment. Resist contrast, γ, is then defined as the slope of T_{norm} on a semi-log scale[5] (*Equation 5*).

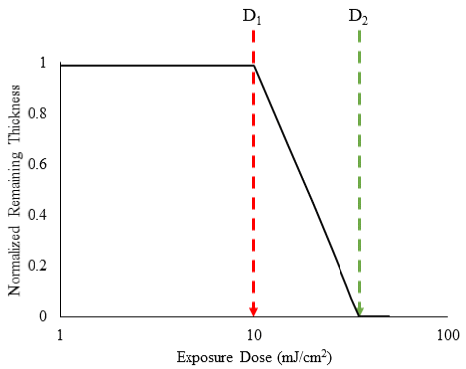

Figure 1. A plot of the remaining film thickness after development as a function of exposure dose. The thickness remaining after development is normalized to the initial thickness prior to development. Exposure dose is given in mJ/cm^2. For doses below a critical value $\mathbf{D_1}$ (red line) the resist thickness is unchanged. For doses above a critical value $\mathbf{D_2}$ (green line) all resist is removed. In-between, thickness decays logarithmically.

$$T_{norm} = \begin{cases} 1 & , \ D < D_1 \\ -\gamma \, \mathrm{Log}_{10}(D) + \gamma \, Log_{10}(D_2), & D_1 < D < D_2 \\ 0 & , \ D_2 < D \end{cases} \quad (4)$$

$$\gamma = \frac{1}{Log_{10}(\frac{D_2}{D_1})} \quad (5)$$

The aerial image contrast, or modulation depth *M*, given by *Equation 3* is set by the exposure optics, and is independent of the photoresist. Due to the partial exposure that may take place in the nulls, aerial image contrast is an important consideration, especially when overexposure is considered. When image contrast is insufficient, the thickness of resist decreases in undesired regions and, in the most extreme case, no pattern remains after development. Using *Equations 3* and *4*, we can calculate the expected sidewall cross section for a single exposed line. An example cross section is plotted in *Figure 2* for $M = 0.98$ and $\gamma = 2.5$. In general, sidewalls will not be perpendicular to the substrate. Therefore, when measuring critical dimensions, the width at the base will be greater than the width at the top. We consider only the width at the base of the pattern for our analysis.

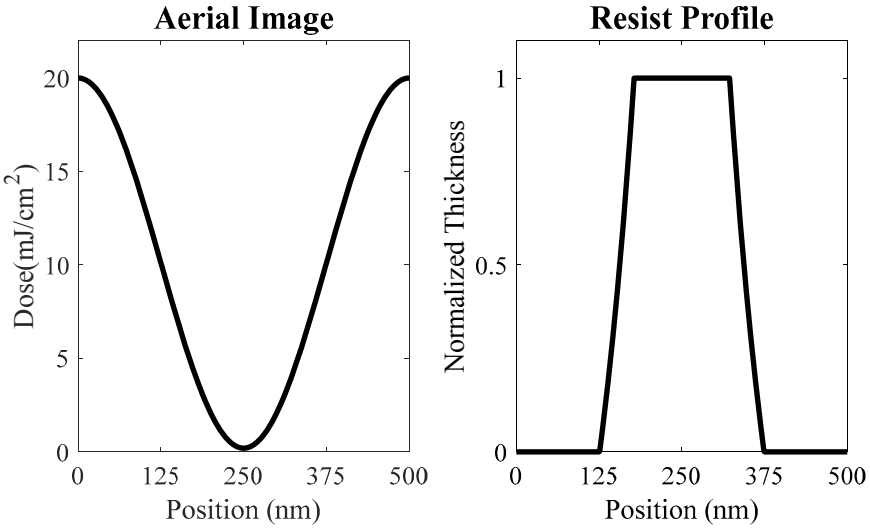

Figure 2. Aerial image (left) and expected resist cross section (right) computed from equation 4. The aerial image has a period of 500 nm, contrast M = 0.98, and a peak dose of 20 mJ/cm^2. The modeled photoresist has a contrast $\gamma = 2.5$, lower threshold $D_1 = 4$ mJ/cm^2, and upper threshold $D_2 = 10$ mJ/cm^2. The resulting cross section after development is normalized to the initial film thickness, and has a width of 250 nm. In the developed cross-section, the sidewalls are not perpendicular to the substrate, so linewidth depends on the height which it is measured. In this paper, linewidth is measured at the base of each feature.

Starting with the work described by Hoffnagle et al[6], we developed a model for linewidth based on both aerial image contrast and resist thresholds and use it to determine the maximum permissible overexposure. Here, the maximum exposure is that which leaves full resist thickness at the center of each feature. This model, detailed in *Equation 6*, gives the minimum remaining linewidth *L*, normalized to the period *Λ*, as a function of thresholds D_1 and D_2 as well as image contrast *M*. We can then define an enhancement factor as the ratio of the half-pitch linewidth to the over-exposed linewidth. *Equation 7* gives the maximum enhancement factor resulting from the maximum overexposure without the dose on line center exceeding $\mathbf{D_1}$.

$$\frac{L}{\Lambda} = 1 - \frac{1}{\pi} \, \mathrm{acos}\left[\frac{D_2}{D_1} \frac{1-M}{M} - \frac{1}{M} \right] \quad (6)$$

$$Enhancement\ Factor = \frac{\Lambda}{2L} = \frac{1}{2}\left(\frac{1}{1-\frac{1}{\pi}\mathrm{acos}\left[\frac{D_2}{D_1}\frac{1-M}{M} - \frac{1}{M} \right]} \right) \quad (7)$$

Both equations can be recast in terms of the resist contrast $\boldsymbol{\gamma}$.

$$\frac{L}{\Lambda} = 1 - \frac{1}{\pi}\,\mathrm{acos}\left[10^{\frac{1}{\gamma}}\,\frac{1-M}{M} - \frac{1}{M}\right] \tag{6}$$

$$Enhancement\ Factor = \frac{\Lambda}{2L} = \frac{1}{2}\left(\frac{1}{1-\frac{1}{\pi}\,\mathrm{acos}\left[10^{\frac{1}{\gamma}}\,\frac{1-M}{M} - \frac{1}{M}\right]}\right) \tag{7}$$

In *Figure 3*, we plot the enhancement factor against both the image contrast M and resist contrast γ**.** As is shown, the enhancement factor improves with increasing image and resist contrasts. Our model can then be used to determine minimum contrast for a given linewidth and pitch. Our model is not complete as there are properties of the photoresist not accounted for which will prevent infinite overexposure at perfect image contrast. Measuring the contrast of various photoresist preparations, we can use *Equation 7* as a starting point for process development.

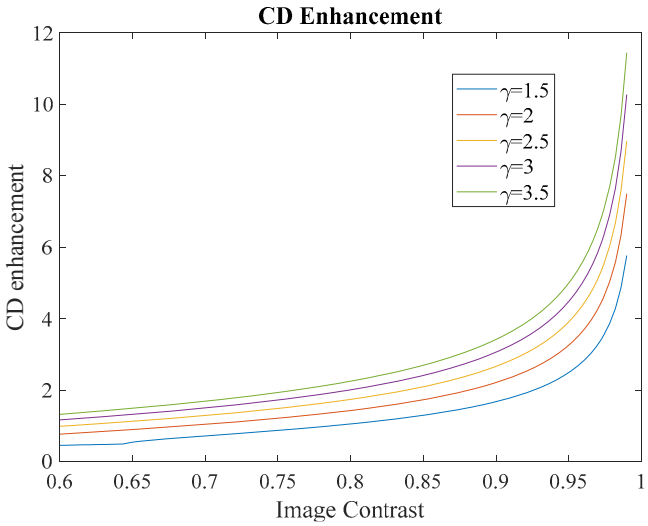

Figure 3. Maximum CD enhancement as a function of aerial image contrast and resist contrast. Curves are plotted from Equation 7. With increasing resist contrast, less image contrast is required to for the same amount of CD enhancement. For significant CD enhancement, very high aerial image contrast is required.

3. METHODS AND MATERIALS

3.1 Materials

We use two commercial resists: Ultra-i 123 (Dow), and AZ 4210 (Merck). Our substrates are Schott NG4 (1.9 mm thick) absorptive filters, chosen to isolate the resist from back reflections. We apply an adhesion promotor, HMDS, to all substrates. Both photoresists are developed with a metal-ion free developer, Microposit MF-319 (Shipley); a 0.24 N aqueous solution of tetra methyl ammonium hydroxide (TMAH).

3.2 Sample Preparation

Schott substrates are prepared by first cleaning the surface with acetone, methanol, Nanostrip, and DI water. Next the substrates are baked on a hotplate at 120 °C for 2 minutes. Once at room temperature, HMDS is spun on at 6000 RPM for 40 seconds. The substrates are then baked again at 120 °C for 2 minutes. The two photoresists (Ultra-i and AZ 4210) are diluted with propylene glycol monomethyl ether acetate (PGMEA) and spin cast onto a substrate. Coating parameters are adjusted to give final film thicknesses (after soft bake) between 120-150 nm. Dilution ratios, spin RPM, spin times, and nominal film thickness for each are given in *Table 1*.

Table 1. Spin coat process parameters. Required dilution ratios, RPM, and spin time vary with each resist.

Resist	Dilution	RPM	Spin Time	Nominal Thickness
AZ 4210	3 : 1	6000	40 s	120 nm
Ultra-i 123	2 : 1	4000	40 s	140 nm

Spin casting is then followed by a pre-exposure bake (soft bake) on a contact hot plate. Soft bake time and temperature for each resist and substrate were optimized for maximum contrast and minimum dark erosion, given a fixed development time of 60 seconds. *Table 2* lists the optimized soft bake time and temperature for each resist on 1.9mm thick NG4 substrates. These parameters will vary with substrate material and geometry.

Table 2. Soft bake process parameters chosen to optimize contrast and minimize dark erosion. All baking is done on a contact hot plate. Optimum parameters are for 1.9 mm thick Schott NG4 substrates. Optimal bake time and temperature will both vary with substrate and resist.

Resist	Bake Temperature	Bake Time
AZ 4210	95°C	45 s
Ultra-i 123	90°C	120 s

3.3. Aerial Image Generation, Resist Exposure and Development

Each aerial image is generated by a Mach-Zehnder interferometer (*Figure 4*) adjusted for spatial period of 500 nm. The light source is an Ar-Ion laser (λ=363.8 nm) with feedback loop to stabilize output power. The beam is polarized, spatially filtered, and collimated to a 4.1 mm diameter. Exposure duration is controlled by a computer controlled shutter. We change optical dose by increasing the exposure time, while holding laser intensity constant. A holographic grating serves as a beam splitter. Each substrate is positioned with a motorized 3 axis stage which allows a series of exposure conditions to be explored on each substrate. All exposures are performed in an environmentally controlled room, with temperature held between 20-24°C and relative humidity between 35-40%. No post exposure bake is used. For all three photoresists, immersion development in MF-319 takes place for 30 seconds at 20°C. After development, the substrates are rinsed with DI water.

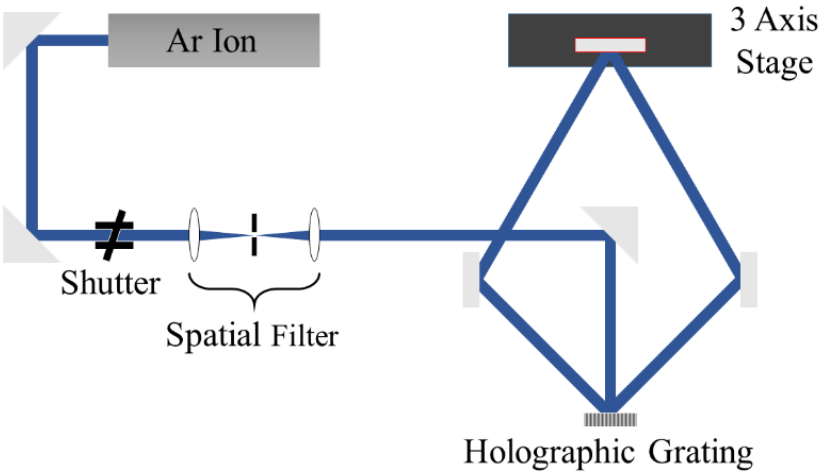

Figure 4. Schematic of interference lithography tool. An Argon Ion laser with λ=363.8 nm (Coherent) provides near TEM_{00} output, with coherence lengths >1 m. The beam is spatially filtered and collimated, then split into symmetric beams with a holographic grating. A substrate coated with photoresist is held by a vacuum chuck on automated positioning stages. The two symmetric laser beams are then interfered in the plane of the substrate. By adjusting mirror position and angle, the interference pitch is adjustable from 200 nm to 2.2 µm. A shutter controls exposure duration.

3.4 Pattern Inspection, Image Processing and Measurement

For inspection, a 2 nm thick layer of platinum is sputtered on top of each sample and the sample is then imaged with a scanning electron microscope. Image processing is performed with SuMMIT software which is used to calculate linewidth, pitch, and line edge roughness for each exposure.

4. RESULTS AND DISCUSSION

Modified processing is required for both photoresists in order to achieve sub 100 nm feature size. The finite aspect ratios supported by the resists require that the films be spun on thinner than is usual in order to achieve <100 nm feature size, leading to the need for dilution with PGMEA. We chose PGMEA because it is the typical delivery vehicle for Novolak based resists. We optimized soft bake parameters for the thinner films. Our finding was that the common rule of thumb, one minute bake per micron, did not apply to such thin films. Following this guideline for <<1 µm films leads to poor adhesion and high dark erosion of the photoresists. For stable, repeatable processing, optimal bake times and temperatures are closer to those for 1µm thick films. We don't use a post exposure bake because we found that the diffusion length of carboxylic acid within the resist often exceeds our feature size. Any post exposure bake erases the patterns. Using a metal ion free developer yields higher pattern contrast with lower line-edge roughness than is typical with potassium hydroxide based developers, such as AZ400K. Immersion development has proven adequate for this R&D work.

Back reflections off of the substrate are problematic for resist exposure. Typically, when working on a reflective substrate, or substrates with large index mismatch, such as silicon, a bottom antireflection coating (BARC) is applied between the substrate and photoresist. So that we can focus only on the resist capabilities and simplify our processing, we use absorptive neutral density filters as a substrate. These are well index-matched to the photoresists and generate very little back reflection – effectively acting as the ultimate BARC. Photoresist adhesion on a glass filter is similar to adhesion on an oxide film on silicon, so much of the work should translate. All threshold dose and contrast measurements are dependent on the substrate material, so proper BARC and soft bake optimization will be required to replicate this work on silicon wafers.

4.1 Minimum CD and Dose Scaling

We exposed each resist with a range of dose to investigate linewidth scaling with dose as well as to find minimum developable feature sizes. In Ultra-i, the smallest features obtained were 50 nm wide with a 500 nm pitch (*Figure 5*). In AZ 4210 the smallest features obtained were 80 nm wide on a 620 nm pitch (*Figure 6*). Both photoresists show similar scaling with exposure dose. Ultra-i linewidth vs dose is plotted in *Figure 7*, and AZ 4210 linewidth vs dose is plotted in *Figure 8*. For both plots, Linewidth is normalized to period and dose is normalized to the dose which corresponds to half pitch feature size. As was expected from analysis of STED techniques, both photoresists exhibit linewidth dose scaling close to $\sqrt{Dose}$. This demonstrates that linewidth can be deterministically controlled across a wide range for a given exposure period. Results from these experiments are summarized in *Table 4*.

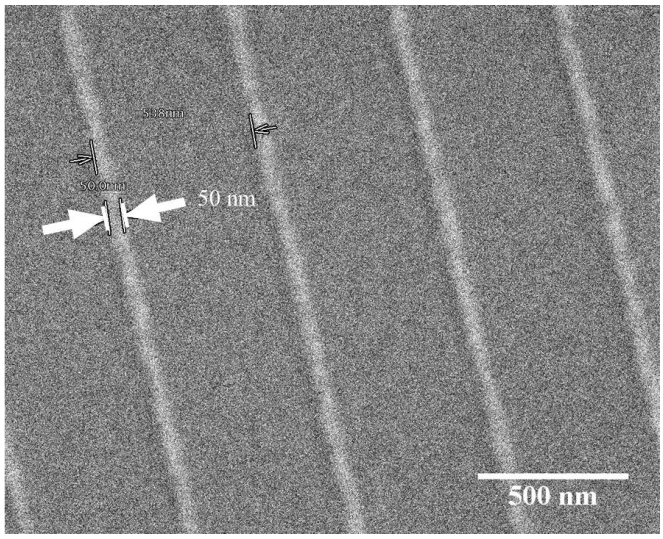

Figure 5. Sub-diffraction features in Ultra-i photoresist. 50 nm wide lines on a 500 nm pitch are demonstrated.

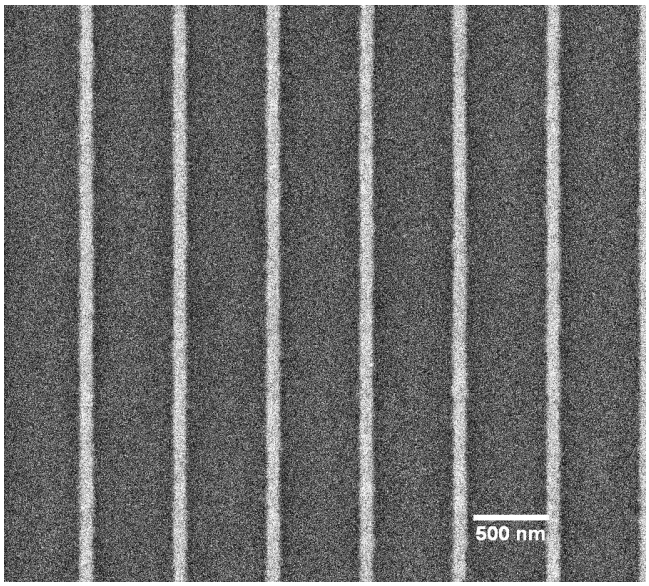

Figure 6. Sub-diffraction features in AZ 4210 photoresist. 80 nm wide lines on 620 nm pitch.

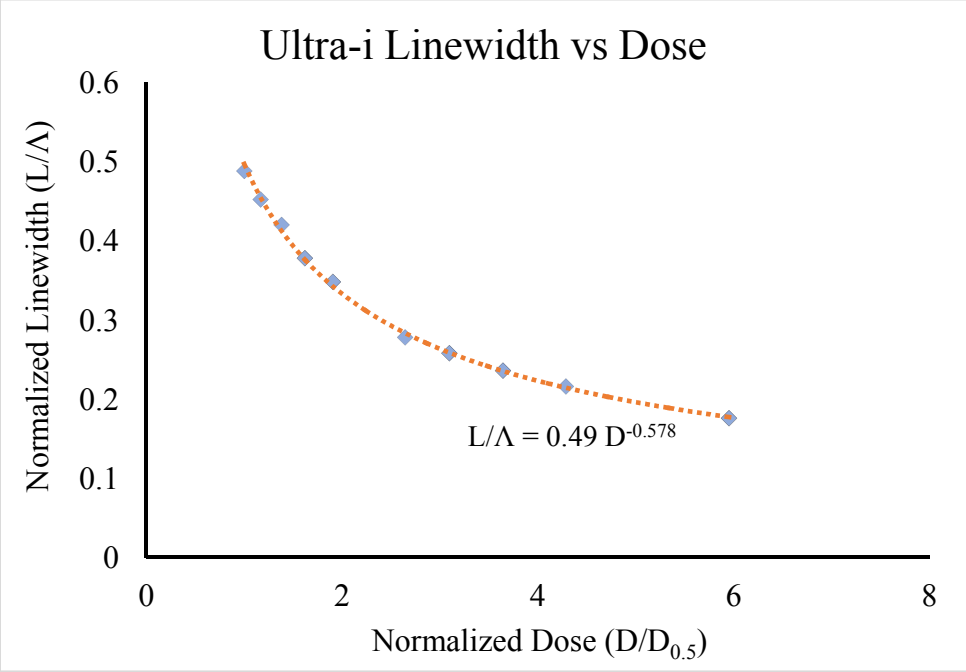

Figure 7. Linewidth as a function of dose in Ultra-i photoresist. The linewidth has been normalized to the pattern period, and the dose is normalized to the dose which results in 1:1 line to space patterns. The measured scaling is close to the expected scaling of $D^{-0.5}$.

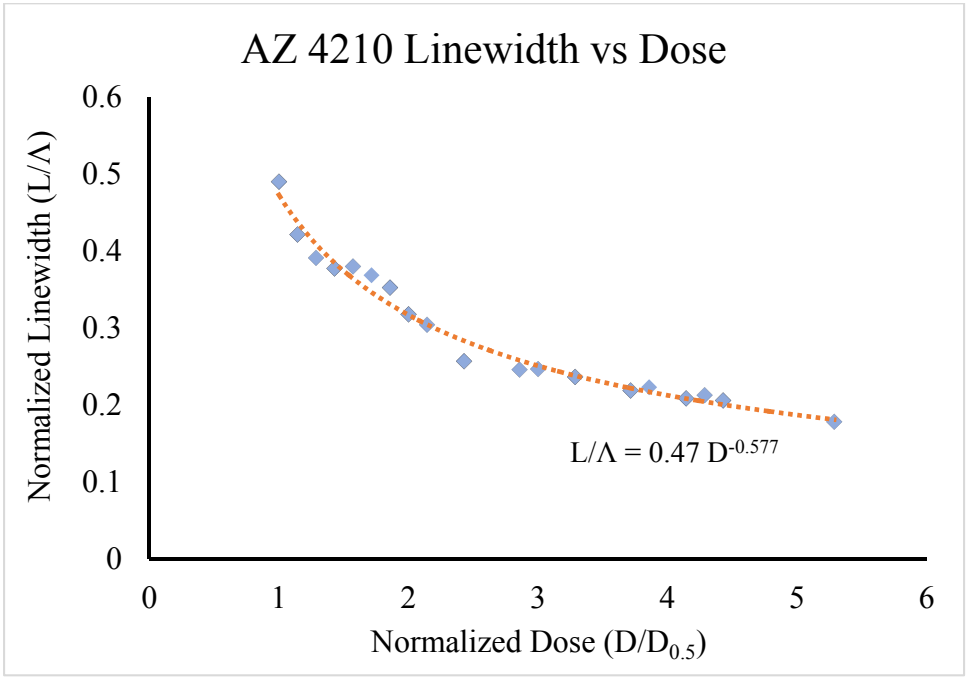

Figure 8. Linewidth as a function of dose in AZ 4210 photoresist. The linewidth has been normalized to the pattern period, and the dose is normalized to the dose which results in 1:1 line to space patterns. The measured scaling is close to the expected scaling of $D^{-0.5}$.

Table 3. Empirically Determined Minimum CD and Scaling Factors.

Resist	Min CD	Dose Scaling Factor
AZ 4210	80 nm	0.578
Ultra-i 123	50 nm	0.577

4.2 Photoresist Contrast Measurements

Using large area exposures, we measured dose thresholds for each resist. Resist films were prepared and developed in the same way as the interference exposures. These test films were exposed with a range of doses using a normal incidence Gaussian beam, diameter = 4.1 mm and power = 1.3 mW. After development, the center of each exposure was inspected to find the minimum dose to initiate development and the minimum dose to complete development. Using these values, the resist contrast was calculated. While the dose thresholds were considerably different for each photoresist, the contrasts were comparable. Dose threshold measurements and the calculated resist contrasts are summarized in *Table 4*.

Table 4. Measured Photoresist Contrast and Dose Thresholds on Schott Filter. Exposed with 4.1 mm Gaussian beam, power = 1.3 mW, peak intensity = 20 mW/cm^2. Developed in MF-319 for 60 seconds (immersion).

Resist	Dose to Initiate (mJ/cm^2)	Dose to Clear (mJ/cm^2)	Contrast
AZ 4210	4 ± 0.6	10 ± 1.5	2.5
Ultra-i 123	11 ± 1.6	28 ± 2.8	2.4

4.3 Line Edge Roughness

A final consideration of great important to lithographers is the line edge roughness (LER) of a pattern. Typically, LER should be no more than 10% of the critical dimension. We measured the LER for various patterns with sub-diffraction critical dimensions. Typical LER for Ultra-i is 5 nm, while typical LER for AZ 4210 is 11 nm. Given this, Ultra-i is suitable for patterns 50nm and larger, while AZ 4210 is only suitable for features larger than 100 nm. Line edge roughness measurements are summarized in *Table 5*.

Table 5. Typical Measured Line Edge Roughness.

Resist	LER (Typical)
AZ 4210	10 nm
Ultra-i 123	5 nm

The photoresist parameters from in Section 4 and the overexposure and development models from Section 2 predict approximately a 6-fold enhancement in CD for both resists. This is in reasonable agreement with our smallest measured features in Ultra-i. In Ultra-i, we achieve 50 nm linewidths on a 500 nm pitch, a 5x enhancement. In AZ 4210, we achieve 80 nm linewidths on a 620 nm pitch, a 4x enhancement. One limitation in our analysis is likely the interference

contrast of the exposure tool. It is difficult to get a direct measure of contrast at the nm scale, but calculating contrast from a tolerance stack up, we estimate the contrast *M~0.98*. Another limitation is the maximum aspect ratio supported by each photoresist. For a given film thickness, this will also set a lower bound on CD. Spinning on thinner resist films may enable smaller critical dimensions. However, reduced film thickness may not always be feasible as subsequent processing determines the minimum required thickness. Not all applications will therefore allow for thinner films.

5. CONCLUSION

We have successfully demonstrated the ability to pattern critical dimensions well below the diffraction limit with conventional far-field i-line photolithography. Standard i-line photoresists combined with modified processing was shown to enable 50 nm critical dimensions. Exposing with a high contrast aerial image, and increasing exposure dose well beyond the nominal dose to clear produces feature sizes well below the diffraction limit. In AZ 4210, the smallest features obtained were 80 nm wide (*Figure 6*). These linewidths correspond to ~λ/4 and are more than 10x smaller than typical critical dimensions that this photoresist is used for. In Ultra-i, the smallest features obtained were 50 nm wide (*Figure 5*). This size corresponds to ~λ/7, and is 5x smaller than the quoted feature size for this material. Linewidths for both photoresist exhibit similar scaling with respect to exposure dose, and are consistent with the expected scaling from STED. From this, deterministic control of linewidth is possible within each exposure. We also find that the line edge roughness is small enough to be about 10% of the minimum feature size obtained of each photoresist.

6. ACKNOWLEDGEMENTS

This work was supported by funding from Sandia National Laboratories as well as NSF MRSEC Grant DMR-1420736. We would like to thank EUV Technology Corporation for providing an academic license to SuMMIT for image analysis. Finally, we would like to acknowledge the resources provided by both the Colorado Nanofabrication Lab and the Colorado Nanomaterials Characterization Facility.

7. REFERENCES

[1] Brunner, T. a., "Why optical lithography will live forever," J. Vac. Sci. Technol. B **21**(6), 2632–2637 (2003).

[2] Rittweger, E., Han, K. Y., Irvine, S. E., Eggeling, C. and Hell, S. W., "STED microscopy reveals crystal colour centres with nanometric resolution," Nat. Photonics **3**(3), 144–147 (2009).

[3] Harke, B., Keller, J., Ullal, C. K., Westphal, V., Schönle, A. and Hell, S. W., "Resolution scaling in STED microscopy," Opt. Express **16**(6), 4154 (2008).

[4] Hazelton, A. J., Wakamoto, S., Hirukawa, S., McCallum, M. and Magome, N., "Double-patterning requirements for optical lithography and prospects for optical extension without double patterning," J. Micro/Nanolithography, MEMS, MOEMS **8**(1), 11003 (2009).

[5] Levinson, H. J., [Principles of Lithography] (2010).

[6] Hoffnagle, J. A., Hinsberg, W. D., Houle, F. A. and Sanchez, M. I., "Characterization of photoresist spatial resolution by interferometric lithography," Metrol. Insp. Process Control Microlithogr., D. J. Herr, Ed., 464 (2003).